




Spectral entropy provides separation between Alzheimer's disease patients and controls: a study of fNIRS

H. Ferdinando^{1,2,a} , S. Moradi³, V. Korhonen^{1,4}, H. Helakari^{1,4}, V. Kiviniemi^{1,4}, and T. Myllylä^{1,3}

¹ Research Unit of Health Sciences and Technology, University of Oulu, 90100 Oulu, Finland

² Department of Electrical Engineering, Petra Christian University, Surabaya 60236, Indonesia

³ Opto-Electronics and Measurement Technique Research Unit, University of Oulu, 90570 Oulu, Finland

⁴ Department of Radiology, Oulu University Hospital, 90100 Oulu, Finland

Received 3 October 2022 / Accepted 28 November 2022 / Published online 19 December 2022
© The Author(s) 2022

Abstract Functional near-infrared spectroscopy (fNIRS) is commonly used as a non-invasive tool to measure cerebral neurovascular dynamics. Its potential for diagnostics of various brain disorders has been already demonstrated in many recent studies, including Alzheimer's disease (AD). fNIRS studies are usually based on comparing hemoglobin measurements at baseline and during a specific task. At present, many proposed methods using fNIRS to diagnose AD involve certain tasks, which may be challenging for the elderly and patients with cognitive decline. Here, we propose a method to characterize AD patients and control in resting state, by applying spectral entropy (SE) analysis on oxyhemoglobin and deoxyhemoglobin, HbO and HbR, respectively, and total hemoglobin (HbT) based on fNIRS signals measured from the left and right sides of the forehead. We applied SE to very low frequency (VLF) (0.008–0.1 Hz), respiratory (0.1–0.6 Hz), and cardiac (0.6–5 Hz) bands to find out which band delivered the optimum result. Next, a *t* test with 0.05 significant level was performed to compare SE values of AD patients and controls. Results from the VLF band looked promising as SE values from AD patients were always significantly higher than those from controls. In addition, this phenomenon was consistent for both sides of the forehead. However, significant differences in SE values in the respiratory band were found from the left hemisphere only, and in the cardiac band from the right hemisphere only. SE value from the VLF band supports a strong argument that it provides good predictability related to the development of AD. We demonstrated that SE of brain fNIRS signal can be an useful biomarker for Alzheimer's disease pathology.

1 Introduction

Alzheimer's disease (AD) is a brain disorder characterized by a cognitive decline due to neuronal degeneration [1]. AD is preceded by amyloid- β and tau-protein accumulation in (peri)arterial brain structures decades before neuronal damage with a spectrum of mild cognitive impairment (MCI) eventually progressing into full dementia in AD. The speed of the progression differs from person to person and early detection would be highly important to be able to start treatments in the early phase to slow down the progression. Recent neuroimaging studies show that an early cognitive decline coincides with changes in the brain cardiovascular pulsatility and permeability of blood–brain barrier (BBB) with respect to the protein accumulations [2–5], which opens an early window into the diagnostics of AD.

Current clinical diagnosis of AD is often based on neurocognitive tests, anatomical magnetic resonance imaging (MRI) [6], nuclear imaging device such as positron emission tomography (PET) and single photon emission computed tomography (SPECT) [7], and biomarker analysis of the cerebrospinal fluid (CSF) samples taken from the patient [8]. Such techniques are labor intensive, requiring clinical laboratories and highly trained persons to perform the study. They also require investments in expensive clinical technology. So, alternatives or supportive methods for the diagnosis, being much easier to perform, would be of high interest.

Functional near-infrared spectroscopy (fNIRS) is commonly used as a non-invasive method to measure blood oxygen saturation (SO₂) and cerebral hemodynamics, for both oxyhemoglobin (HbO) and deoxyhemoglobin (HbR). By summing HbO and HbR, we can provide total hemoglobin (HbT). The fNIRS method is

^a e-mail: hany.ferdinando@oulu.fi (corresponding author)

based on illumination of light to the scalp using two or more wavelengths selected from both sides of the isosbestic point of blood at around 800 nm. Next, the absorption changes of the detected back-scattered light, which has reached the brain at a maximum penetration depth of approximately 1–2 cm [9], are used to quantify the hemodynamic changes [9]. fNIRS is not a new technique to study AD. In 1996, Hock et al. published their work on monitoring HbO and HbT changes in the frontal cortex during a verbal fluency task (VFT) [10]. Later, Fallgatter et al. reported a loss of functional hemispheric asymmetry in Alzheimer-type dementia during VFT using fNIRS from the frontal cortex area [11]. In addition, Fladby et al. investigated the olfactory response in the early stages of AD using fNIRS [12]. Other researchers also demonstrated that fNIRS is a promising technique to study the early detection of AD [13–17]. The abovementioned articles involved certain tasks during their studies. Although we can standardize the tasks, it does not guarantee that everybody does them correctly, especially in the case of elderly and AD patients. So, having measurements without the need for specific tasks would be preferable.

Spectral entropy (SE) is a measure of spectral power distribution of a signal based on the Shannon entropy [18], or a form of Shannon entropy normalized with power spectrum amplitude [19]. SE reflects the flatness or complexity of the signal's spectrum [20–22]. Hence, SE calculation starts from normalized power spectral density (PSD). There are many methods to get PSD, e.g., fast Fourier transform (FFT) and periodogram. Based on the nature of spectral entropy, a signal with a flat spectrum should have a maximal SE value [23]. Using SE to analyze signals neglects the order of frequency appearance in the time domain. It means different orders of frequency appearance will have the same SE value as long as the frequency contents remain the same. SE is commonly used in biosignal analysis, particularly in electroencephalography (EEG).

A recent study used SE to explore electrophysiological and hemodynamic changes in the drug-resistant epilepsy (DRE) [18] and showed that the dynamic spatiotemporal features of multimodal SE provided a marker to separate DRE from healthy controls. Specific for hemodynamics, SE of DRE patient was always less than that of controls, but the significant differences varied among different bands and concentrations. Helakari et al. applied SE to fast functional MRI (fMRI) and EEG signals during sleep study and found that spectral entropy decreases in the VLF and respiratory bands [24]. Sharma et al. used SE as one of the features extracted from EEG to separate MCI, dementia, and controls using support vector machine (SVM) [25]. The proposed system achieved accuracy of up to 90%. In addition, SE was also applied to magnetoencephalography (MEG) among MCI, AD, and controls [26]. Bruña et al. found that based on the MEG signal analysis, the abnormality degree of MCI was between AD and controls [27]. Here, we propose fNIRS technique to characterize AD patients and controls by applying SE without



Fig. 1 Two fNIRS channels (optodes) were placed on forehead on left (L) and right (R) side

a need to perform specific tasks during measurements; hence, subjects are measured in resting state.

2 Materials and methods

2.1 fNIRS device

Our fNIRS device uses wavelengths of 690 nm and 830 nm and a frequency-coding technique to label them for detection, and lock-in amplification with a very narrow bandwidth filter in the receiver to minimize noise [28]. At the detection part, signals followed by a transimpedance amplifier (TIA) are digitized by a DAQ card at 800 Hz. Next, the digital signal is fed into a digital lock-in detection circuit to detect the coded frequency and remove unwanted noise. Light illumination and detection on the human head were realized by optical fibers fabricated by Schott and customized for this study by Fiberoptics Technology. The fiber tips (with a diameter of 2.5 mm) were attached to the head by a plastic fiber clip at a 3 cm fiber source-detector distance, to ensure penetration depth up to the brain tissue, see Fig. 1.

2.2 Measurement protocol

The data collection followed the guidelines established by the Declaration of Helsinki. All measurements took place in Oulu University Hospital, Oulu, Finland. This study was approved by the regional Ethical Committee of Northern Ostrobothnia Hospital District in Oulu University Hospital. This study involved 8 patients (62.6 ± 2.1 -year-old) with diagnosed AD and 14 age-matched controls (63.6 ± 2.9 -year-old). All participants signed informed consent letters before the measurements. Most of the participants also filled out the minimal state exam (MMSE) prior to the measurements.

Table 1 Subject characteristics

	AD patients	Controls
Number of participants (female)	8 (5, 63%)	14 (6, 43%)
Age	62.6 ± 2.1	63.6 ± 2.9
Minimum age	60	52
Maximum age	65	67
MMSE (mean ± SD)	22.8 ± 1.6	28.5 ± 1.5
Minimum MMSE score	19	25
Maximum MMSE score	27	30

Based on the MMSE score, AD patients who participated in this study were in the mild dementia stage, see Table 1. All the patients have undergone routine AD clinical evaluation (neurocognitive tests and MRI) and some cases with also CSF tau and beta-amyloid evaluation.

During measurement, all participants were in a supine position, and scanned simultaneously by fMRI and fNIRS. Simultaneous measurements of fNIRS and fMRI were taken place for 5 min in the resting state. This study focuses on the use of fNIRS only; however, signal quality of the fNIRS device was verified by the blood oxygen level dependent (BOLD) signal provided by the fMRI [28].

2.3 Signal analysis

Modified Beer-Lambert law (MBLL) was used to calculate concentration changes of HbO, HbR, with the following coefficients: 690 nm: 0.3123 for HbO and 2.1382 for HbR, 830 nm: 1.0507 for HbO and 0.7804 for HbR, with differential path length factor of 5.93 [29]. Prior to signal analysis, calculated HbO, HbR, and HbT signals were downsampled at 10 Hz to fit the sampling frequency of the ultra-fast fMRI [30]. The fNIRS analysis was performed in the very low frequency (VLF) (ranging from 0.008 to 0.1 Hz), respiratory (ranging from 0.1 to 0.6 Hz), and cardiac (ranging from 0.6 to 5 Hz) bands [31], and for these filtered bands, we calculated the SE using *pentropy* function in Matlab™ 2022a by setting the instantaneous parameter to false to get a single number. Finally, we used a *t* test at a significant level of 0.05 to evaluate whether the SE of AD patients was different when compared to controls.

3 Results

Figure 2 shows the average normalized spectra of HbO, HbR, and HbT measured from AD patients (on the left) and controls (on the right). As can be seen, there are visible differences between the two spectra.

In the following, Figs. 3, 4 and 5 present comparisons of SE values of HbO, HbR, and HbT between controls

and AD patients. Three frequency bands are included when fNIRS measures from the left (L) and right (R) sides of the forehead (Fig. 1).

SE results show that, in the VLF band, all concentrations can deliver significant differences on both sides of the forehead. In addition, SE values from AD patients in both VLF and respiratory bands are always higher than controls. On the other hand, the opposite occurred for SE values in the cardiac band.

Figure 6 displays plots of MMSE against SE values in the VLF band of HbO, HbR, and HbT, from both left and right. The best fit line in each panel indicates decreasing trend as MMSE is increasing.

4 Discussion

This is the first study to show that SE of the human brain fNIRS signals from AD patients is significantly different from controls. Furthermore, the SE values in the VLF band decreases as the MMSE scores increases indicating its potential for a neurocognitive biomarker in AD. AD patients have significantly higher SE values in the VLF band in all measured markers, i.e., HbO, HbR, and HbT. In addition, the respiratory and cardiovascular bands were altered but not as clearly as the VLF band. SE values in the VLF band have a small standard deviation indicating high consistency further supporting the notion that SE values in the VLF band can be a good biomarker for AD.

The high SE values indicate high-frequency variance in the signal. VLF (0.008–0.1 Hz) band corresponds to vasomotor brain waves, which originate from the vasomotor tone of arterial wall smooth muscle cells controlling the luminal diameter. Vasomotor activity controls the regional blood flow with diameter changes affecting the flow resistance, and thus it is reflected in the flow and blood volume in the vascular tree, ranging from arteries to capillaries and veins [32]. These results indicate that AD patients have significantly more variations in vascular diameter than controls do.

The finding of altered variance in the brain pulsations is in line with the recent studies indicating altered variance of the blood flow, blood–brain permeability, and cardiovascular pulse propagation in the brain [2, 3, 31]. Furthermore, in AD, the amyloid proteins accumulated in the walls of arteries may alter the vasomotor function, as shown in the IPAD intramural accumulation of amyloid in AD [33]. The pulsations drive brain clearance of protein waste, and the failure of brain waste clearance precedes neurodegenerative tissue changes.

It has been shown that AD is linked to rising blood pressure that increases the stiffness of blood wall structure reflected as a loss of neurovascular autoregulation and vasodilatory activation responses [34]. As the brain has a vast vascular content, especially in grey matter, the brain tissue elasticity is also affected by the VLF vasomotor wave disturbances [35].

Fig. 2 Average normalized spectra of HbO, HbR, and HbT from AD patients and controls

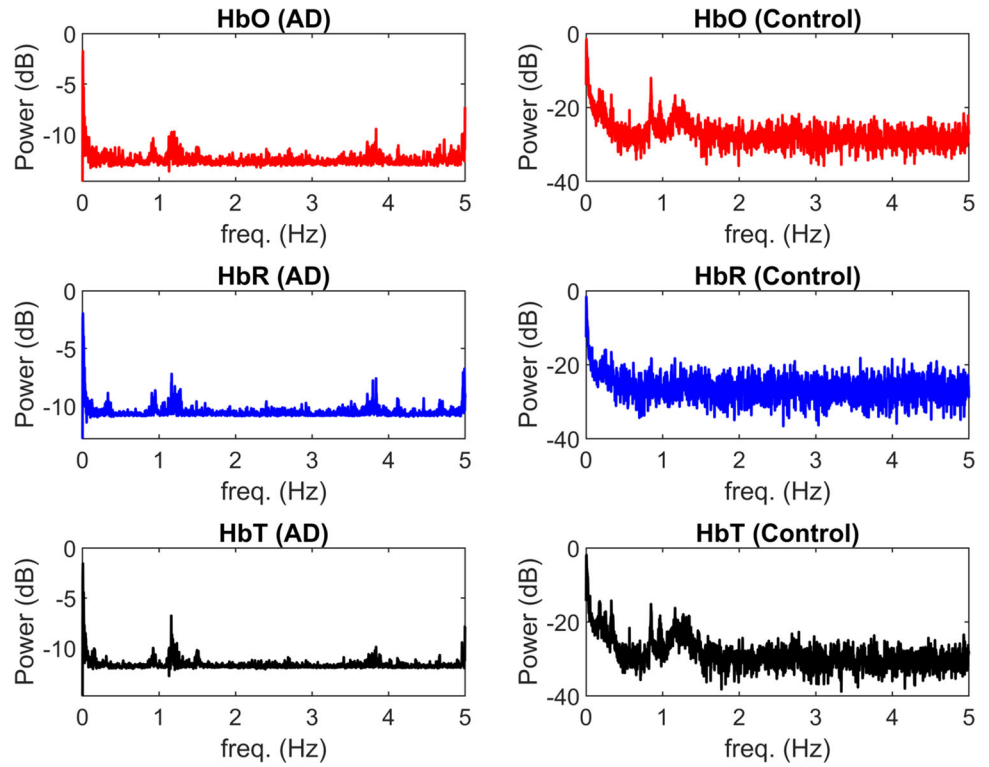


Fig. 3 VLF band bar charts of HbO, HbR, and HbT show that SE from controls and AD patients are significantly different; *L* left, *R* right

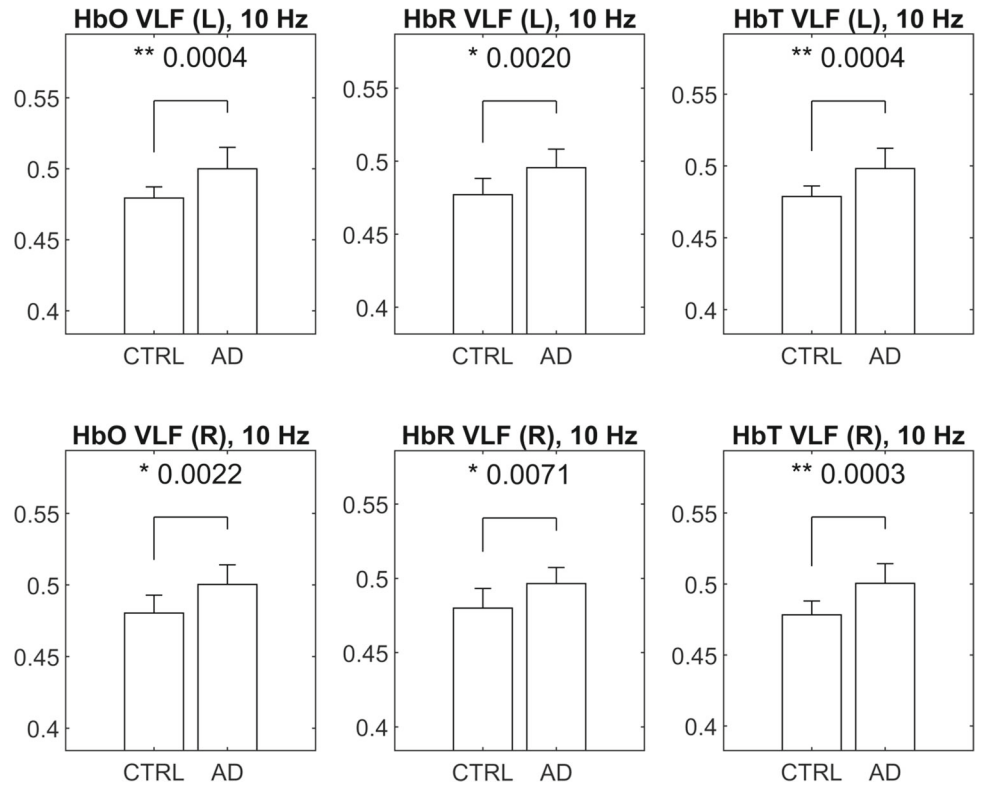


Fig. 4 Respiratory band bar charts of HbO, HbR, and HbT show that SE from controls and AD patients are significantly different only for the left side; *L* left, *R* right

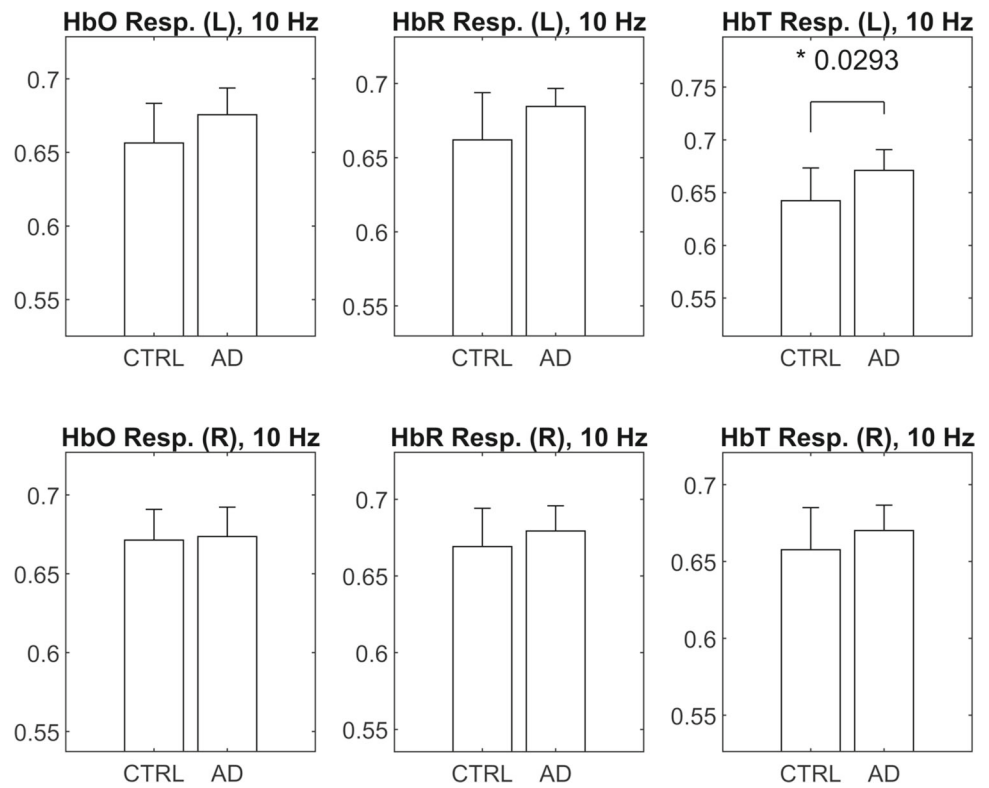


Fig. 5 Cardiac band bar charts of HbO and HbR show that SE from controls and AD patients are significantly different only for the right side; *L* left, *R* right

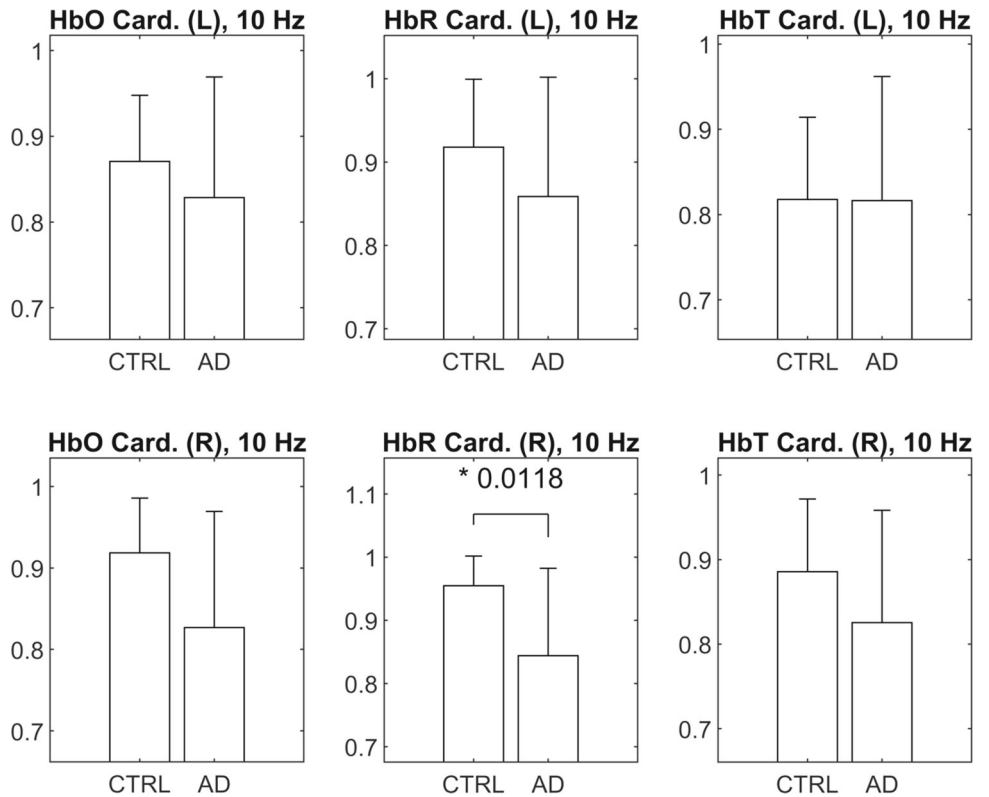
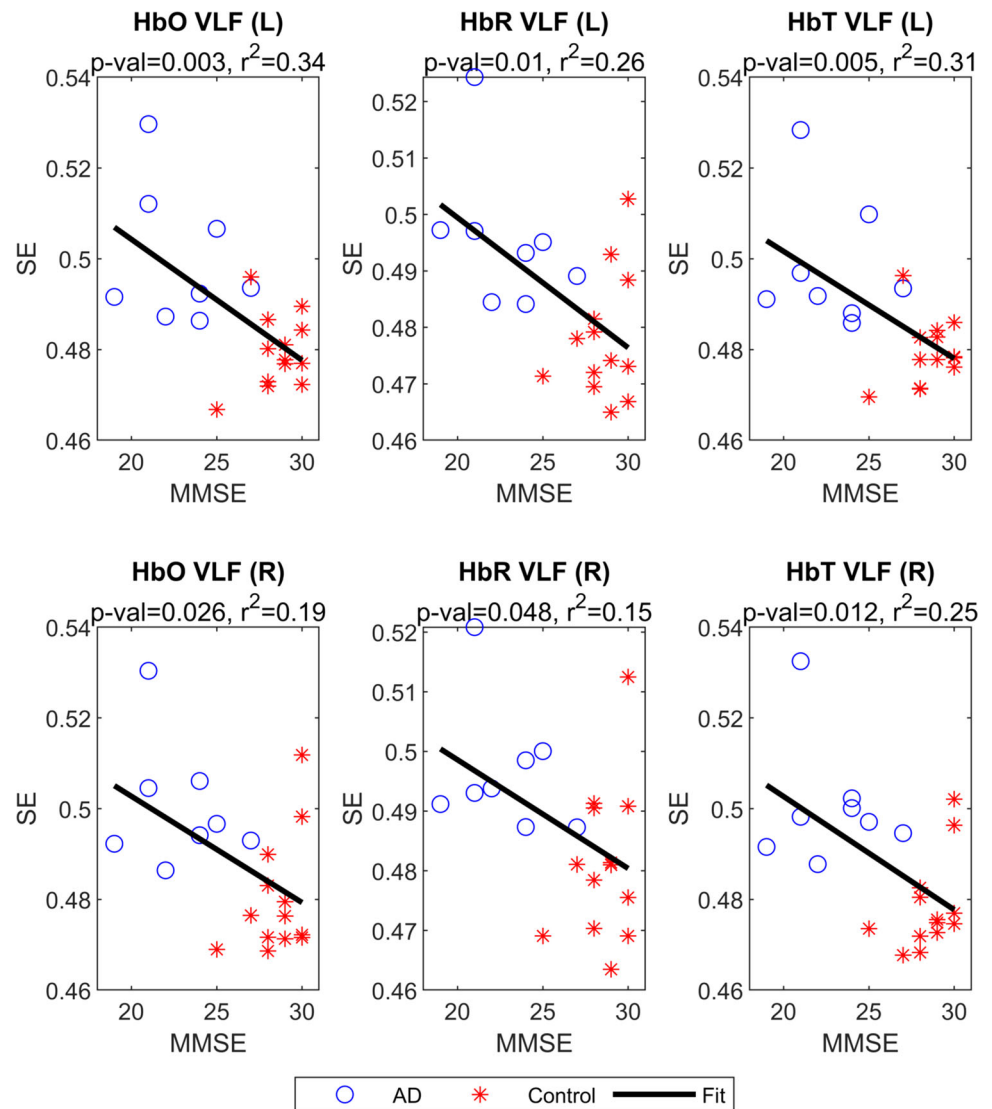


Fig. 6 Plots of MMSE vs. SE in VLF band



AD is also associated with sleep disordered breathing (SDB) [36, 37] with a prevalence of over 50% [38]. People with SDB experience cognitive impairments such as attention deficits and memory loss [39], which correlate with neuroanatomical changes and grey matter loss [40]. Interestingly, SDB also advances cognitive decline in the elderly [41] and obstructive sleep apnea (OSA) links to neurophysical scores for various brain functions [42]. Specific to the frontal cortex where we measured the hemodynamic response, this part is highly associated with memory, attention, and higher cognitive function [43] as has been found in AD patients. Although we did not assess if our subjects experienced SDB, our finding in the respiratory band seems to support the relationship between AD and SDB.

The anatomical MRI analysis of our AD patients detected no lesions in the measurement area of the NIRS. However, we found one small individual lacuna

infarct from two patients (in insula and in right parietal sensory cortex), one meningioma 8 mm in opposing parietal cortex and 4 mm subcortical microhaemorrhages in upper premotor area. These should have no effect to NIRS signal. Hippocampal atrophy varied from grades 0 to 3, and cortical atrophy was mostly mild (6/8, maximum grades 1) suiting the high MMSE scores of our AD cases. There were also some white matter hyperintensities, but these did not reach the frontal cortex where NIRS was reading the signal either.

Results in the respiratory bands showed that SE values of AD patient are always larger than those of controls in all concentrations and bands. However, significant differences of SE value in respiratory band were found from the left hemisphere only due to a large variation or standard deviation. In the cardiac band, the SE values of AD are smaller than those of controls in all concentrations. These facts encourage to have further analysis using more data.

The best fit lines in Fig. 6 show a decreasing trend as the MMSE value increases. It supports a strong argument that SE in the VLF band provides good predictability related to the development of AD. In other words, it reflects the progression of AD. Based on Table 1, all AD patients who participated in this study were in mild or early form of dementia. Hence, the difference between AD patients and controls should be small. However, SE value in VLF band demonstrated significant difference between these two groups, showing the potential of this method for early detection of glymphatic failure in AD, e.g., using SE values to classify severe, moderate, and mild dementia.

Although the proposed method looked promising, this finding may be somewhat limited by the small number of subjects. The balance between AD patients and controls may also add another limitation. In the future studies, we will have more subjects involved, we can estimate the diagnostic accuracy and SE characteristic among different sex, age, etc., groups.

In conclusion, we show that the SE of brain fNIRS signal can be a useful biomarker for Alzheimer's disease pathology. The proposed method can be used as a preliminary diagnosis tool prior to more thorough evaluations using the abovementioned ones.

Acknowledgements The authors would like to acknowledge Academy of Finland, Grant/Award numbers: 318347, 338599, TERVA 314497, TERVA 335720; Jane ja Aatos Erkkö Foundation; Riitta and Jorma J. Takanen foundation; Business Finland Grant (42539/31/2020) and Infotech for financing this research.

Funding Information Open Access funding provided by University of Oulu including Oulu University Hospital.

Open Access This article is licensed under a Creative Commons Attribution 4.0 International License, which permits use, sharing, adaptation, distribution and reproduction in any medium or format, as long as you give appropriate credit to the original author(s) and the source, provide a link to the Creative Commons licence, and indicate if changes were made. The images or other third party material in this article are included in the article's Creative Commons licence, unless indicated otherwise in a credit line to the material. If material is not included in the article's Creative Commons licence and your intended use is not permitted by statutory regulation or exceeds the permitted use, you will need to obtain permission directly from the copyright holder. To view a copy of this licence, visit <http://creativecommons.org/licenses/by/4.0/>.

Data availability statement Data cannot be made available for public because we do not have permission to share raw data.

Declarations

Conflict of interest The authors have no conflict of interest.

References

1. Alzheimer's Association, *Alzheimer's Disease Facts and Figures* (Alzheimer's Association, Chicago, 2022), p.2022
2. D.A. Nation, M.D. Sweeney, A. Montagne, A.P. Sagare, L.M. D'Orazio, M. Pachicano et al., Blood–brain barrier breakdown is an early biomarker of human cognitive dysfunction. *Nat. Med.* **25**(2), 270–276 (2019)
3. Z. Rajna, H. Mattila, N. Huotari, T. Tuovinen, J. Krüger, S.C. Holst et al., Cardiovascular brain impulses in Alzheimer's disease. *Brain* **144**, 2214–2226 (2021)
4. R. Aldea, R.O. Weller, D.M. Wilcock, R.O. Carare, G. Richardson. Cerebrovascular smooth muscle cells as the drivers of intramural periarterial drainage of the brain. *Front. Aging Neurosci.* **11**(1) (2019)
5. G. Barisano, A. Montagne, K. Kisler, J.A. Schneider, J.M. Wardlaw, B.V. Zlokovic, Blood–brain barrier link to human cognitive impairment and Alzheimer's disease. *Nat. Cardiovasc. Res.* **1**(2), 108–115 (2022)
6. J. Nedelec, N. Bolo, Y. Hodé, J. Macher, Alzheimer's disease: potential of imaging and spectroscopic techniques: PET, SPECT, DCS-MRI, MRI, MRS and fMRI an overview. *Eur. Psychiatry* **13**, 168s–s169 (1998)
7. K. Pietrzak, K. Czarnecka, E. Mikiciuk-Olasik, P. Szymanski, New perspectives of Alzheimer disease diagnosis—the most popular and future methods. *Med. Chem.* **14**, 34–43 (2018)
8. H.M. Chapel, M.M. Esiri, G.K. Wilcock, Immunoglobulin and other proteins in the cerebrospinal fluid of patients with Alzheimer's disease. *J. Clin. Pathol.* **37**, 697–699 (1984)
9. D.A. Boas, C.E. Elwell, M. Ferrari, G. Taga, Twenty years of functional near-infrared spectroscopy: introduction for the special issue. *Neuroimage* **85**, 1–5 (2014)
10. C. Hock, K. Villringer, F. Müller-Spahn, M. Hofmann, S. Schuh-Hofer, H. Heekeren et al., Near infrared spectroscopy in the diagnosis of Alzheimer's disease. *Ann. N. Y. Acad. Sci.* **777**, 22–29 (1996)
11. A.J. Fallgatter, M. Roesler, L. Sitzmann, A. Heidrich, T.J. Mueller, W.K. Strik, Loss of functional hemispheric asymmetry in Alzheimer's dementia assessed with near-infrared spectroscopy. *Cogn. Brain Res.* **6**, 67–72 (1997)
12. T. Fladby, G. Bryhn, O. Halvorsen, I. Rosé, M. Wahlund, P. Wiig et al., Olfactory response in the temporal cortex of the elderly measured with near-infrared spectroscopy: A preliminary feasibility study. *J. Cereb. Blood Flow Metab.* **24**, 677–680 (2004)
13. S. Jahani, A.L. Fantana, D. Harper, J.M. Ellison, D.A. Boas, B.P. Forester et al., fNIRS can robustly measure brain activity during memory encoding and retrieval in healthy subjects. *Sci. Rep.* **7**, 1–14 (2017)
14. R. Li, G. Rui, W. Chen, S. Li, P.E. Schulz, Y. Zhang, Early detection of Alzheimer's disease using non-invasive near-infrared spectroscopy. *Front. Aging Neurosci.* **10**, 1–11 (2018)
15. D. Perpetuini, A.M. Chiarelli, D. Cardone, C. Filippini, R. Bucco, M. Zito et al., Complexity of frontal cortex fNIRS can support Alzheimer disease diagnosis in memory and visuo-spatial tests. *Entropy* **21**, 26 (2019)
16. D. Yang, R. Huang, S.H. Yoo, M.J. Shin, J.A. Yoon, Y.I. Shin et al., Detection of mild cognitive impairment using convolutional neural network: temporal-feature maps

- of functional near-infrared spectroscopy. *Front. Aging Neurosci.* **12**, 141 (2020)
17. J. Kim, D.K. Yon, K.Y. Choi, J.J. Lee, N. Kim, K.H. Lee et al., Novel diagnostic tools for identifying cognitive impairment using olfactory-stimulated functional near-infrared spectroscopy: patient-level, single-group, diagnostic trial. *Alzheimers Res. Ther.* **14**, 1–10 (2022)
 18. H. Helakari, J. Kananen, N. Huotari, L. Raitamaa, T. Tuovinen, V. Borchardt et al., Spectral entropy indicates electrophysiological and hemodynamic changes in drug-resistant epilepsy—a multimodal MREG study. *Neuroimage Clin.* **22**, 101763 (2019)
 19. U.R. Acharya, H. Fujita, V.K. Sudarshan, S. Bhat, J.E.W. Koh, Application of entropies for automated diagnosis of epilepsy using EEG signals: a review. *Knowl. Based Syst.* **88**, 85–96 (2015)
 20. A. Vakkuri, A. Yli-Hankala, P. Talja, S. Mustola, H. Tolvanen-Laakso, T. Sampson et al., Time-frequency balanced spectral entropy as a measure of anesthetic drug effect in central nervous system during sevoflurane, propofol, and thiopental anesthesia. *Acta Anaesthesiol. Scand.* **48**, 145–153 (2004)
 21. N. Zaccarelli, B.L. Li, I. Petrosillo, G. Zurlini, Order and disorder in ecological time-series: Introducing normalized spectral entropy. *Ecol. Indic.* **28**, 22–30 (2013)
 22. J. Sun, B. Wang, Y. Niu, Y. Tan, C. Fan, N. Zhang et al., Complexity analysis of EEG, MEG, and fMRI in mild cognitive impairment and Alzheimer’s disease: a review. *Entropy* **22**, 239 (2020)
 23. X. Yu, Z. Mei, C. Chen, W. Chen, Ranking power spectra: a proof of concept. *Entropy* **21**, 1057 (2019)
 24. H. Helakari, V. Korhonen, S.C. Holst, J. Piispala, M. Kallio, T. Väyrynen et al., Human NREM sleep promotes brain-wide vasomotor and respiratory pulsations. *J. Neurosci.* **42**(12), 2503–2515 (2022)
 25. N. Sharma, M.H. Kolekar, K. Jha, Y. Kumar, EEG and cognitive biomarkers based mild cognitive impairment diagnosis. *IRBM* **40**, 113–121 (2019)
 26. A.L. Fred, S.N. Kumar, A.K. Haridhas, S. Ghosh, H.P. Bhuvana, W.K.J. Sim et al., A brief introduction to magnetoencephalography (MEG) and its clinical applications. *Brain Sci.* **12**, 788 (2022)
 27. R. Bruña, J. Poza, C. Gómez, M. García, A. Fernández, R. Hornero, Analysis of spontaneous MEG activity in mild cognitive impairment and Alzheimer’s disease using spectral entropies and statistical complexity measures. *J. Neural Eng.* **9**, 036007 (2012)
 28. H. Sorvoja, T. Myllylä, M.Y. Kirillin, E.A. Sergeeva, R.A. Myllylä, A.A. Elseoud et al., Non-invasive, MRI-compatible fibreoptic device for functional near-IR reflectometry of human brain. *Quantum Electr. (Woodbury)* **40**, 1067–1073 (2020)
 29. M. Cope. *The Application of Near Infrared Spectroscopy to Non Invasive Monitoring of Cerebral Oxygenation in the Newborn Infant* (Doctoral Thesis. University College London, 1991).
 30. V. Korhonen, T. Hiltunen, T. Myllylä, X. Wang, J. Kantola, J. Nikkinen et al., Synchronous multiscale neuroimaging environment for critically sampled physiological analysis of brain function: hepta-scan concept. *Brain Connect.* **4**, 677–689 (2014)
 31. T. Tuovinen, J. Kananen, Z. Rajna, J. Lieslehto, V. Korhonen, R. Rytty et al., The variability of functional MRI brain signal increases in Alzheimer’s disease at cardiorespiratory frequencies. *Sci. Rep.* **10**(1), 1–11 (2020)
 32. M. Fog, Vasomotor reactions, especially in view of physiology and methods. *Acta Psychiatr. Scand.* **14**, 11–13 (1939)
 33. C.A. Hawkes, N. Jayakody, D.A. Johnston, I. Bechmann, R.O. Carare, Failure of perivascular drainage of β -amyloid in cerebral amyloid angiopathy. *Brain Pathol.* **24**(4), 396–403 (2014)
 34. C.S. Roy, C.S. Sherrington, On the regulation of the blood-supply of the brain. *J. Physiol.* **11**, 85–108 (1890)
 35. S.J. van Veluw, S.S. Hou, M. Calvo-Rodriguez, M. Arbel-Ornath, A.C. Snyder, M.P. Frosch et al., Vasomotion as a driving force for paravascular clearance in the awake mouse brain. *Neuron* **105**(3), 549–561.e5 (2020)
 36. T.K. Ulland, A.C. Ewald, A.O. Knutson, K.M. Marino, S.M.C. Smith, J.J. Watters, Alzheimer’s disease, sleep disordered breathing, and microglia: puzzling out a common link. *Cells* **10**, 2907 (2021)
 37. C. André, S. Rehel, E. Kuhn, B. Landeau, I. Moulinet, E. Touron et al., Association of sleep-disordered breathing with Alzheimer disease biomarkers in community-dwelling older adults: a secondary analysis of a randomized clinical trial. *JAMA Neurol.* **77**, 716–724 (2020)
 38. D.L. Bliwise, Sleep disorders in Alzheimer’s disease and other dementias. *Clin. Cornerstone* **6**, S16–28 (2004)
 39. M.L. Jackson, M.E. Howard, M. Barnes, Cognition and daytime functioning in sleep-related breathing disorders, in *Progress Brain Research*, vol. 190, 1st edn., ed. by S.G. Waxman, D.G. Stein, D.F. Swaab, H.L. Fields (Elsevier, Amsterdam, 2011), pp.53–68
 40. M.E. Zimmernan, M.S. Aloia, A review of neuroimaging in obstructive sleep apnea. *J. Clin. Sleep Med.* **2**, 461–471 (2006)
 41. R.S. Osorio, T. Gumb, E. Pirraglia, A.W. Varga, S.E. Lu, J. Lim et al., Sleep-disordered breathing advances cognitive decline in the elderly. *Neurology* **84**, 1964–1971 (2015)
 42. E.K. Stranks, S.F. Crowe, The cognitive effects of obstructive sleep apnea: an updated meta-analysis. *Arch. Clin. Neuropsychol.* **31**, 186–193 (2016)
 43. S. Celle, R. Peyron, I. Faillenot, V. Pichot, M. Alabdullah, J.M. Gaspoz et al., Undiagnosed sleep-related breathing disorders are associated with focal brainstem atrophy in the elderly. *Hum. Brain Mapp.* **30**, 2090–2097 (2009)